Synthesis and Photo-Induced Electron Transfer Reactions in a $La_2@I_h$-C_{80}–Phenoxazine Conjugate

Takeshi Akasaka,*[a,b,c,d] Akira Nakata,[a] Marc Rudolf,[e] Wei-Wei Wang,[f] Michio Yamada,[d] Mitsuaki Suzuki,[d] Yutaka Maeda,[d] Ryo Aoyama,[a] Takahiro Tsuchiya,[a] Shigeru Nagase,*[f] and Dirk M. Guldi*[e]

Abstract: A newly designed electron donor–acceptor conjugate consisting of an endohedral dimetallofullerene ($La_2@I_h$-C_{80}) and phenoxazine (POZ) was successfully synthesized by exploiting Prato conditions. Our results document that the 1,3-dipolar cycloaddition took place across the [5,6] junction to afford exclusively the corresponding [5,6]-cyloadduct. The structure of the conjugate was characterized by means of NMR spectroscopy, absorption spectroscopy, and electrochemical studies. Computational calculations suggest that the HOMO is distributed on the POZ moiety whereas the LUMO is located at the endohedral La atoms, leading to efficient separation of the HOMO and LUMO in the conjugate. Time-resolved absorption spectroscopic investigations and spectroelectrochemical measurements corroborate the formation of the energetically low-lying $(La_2@I_h\text{-}C_{80})^{\bullet-}$-$(POZ)^{\bullet+}$ radical ion pair state via ultrafast through-space electron transfer.

Introduction

A variety of electron donor–acceptor (D–A) conjugates have been designed and synthesized for artificial photosynthesis and photovoltaics in the field of solar energy conversion schemes.[1] Particularly, fullerene have been recognized as an excellent electron acceptor.[2] Owing to its three-dimensional rigid structure, C_{60} – the most abundant fullerene – possesses small reorganization energy in charge transfer reactions, which plays an important role in efficient and fast charge separation as well as slow charge recombination. In addition, C_{60} has high electron affinity and features high carrier transport properties.[3] To date, a large number of electron D–A conjugates, where an electron donor is combined with C_{60}, have been prepared and their photoinduced electron transfer properties have been explored.[4]

Recently, another class of fullerenes, namely endohedral metallofullerenes

(EMFs)[5], has gained interest as an alternative component for such D–A conjugates.[6] As a matter of fact, the electronic properties of EMFs differ greatly from that of C_{60} and depend on the fullerene size, on one hand, and the encaged metal species, on the other hand. For example, a dimetallic EMF, $M_2@I_h$-C_{80} (M = La or Ce) undergoes much easier reduction and oxidation than C_{60}.[7] Therefore, from an electrochemical perspective, $M_2@I_h$-C_{80} is likely to serve as either an electron acceptor or an electron donor. Recent advances in the field have shown that $La_2@I_h$-C_{80} act as an electron acceptor in the excited state, when, for example, combined with extended tetrathiafulvalene (exTTF) via a 5,6-pyrrolidine ring[6d] (**1**; see Figure 1). In this particular case, photo-excitation of **1** is the inception to a fast charge separation resulting in the formation of a 3.2 ns lived radical ion pair in toluene. It is also noteworthy that switchable charge transfer events were found when zinc tetraphenylporphyrin (ZnP), a weaker electron donor than exTTF, was attached to $M_2@I_h$-C_{80} (M = La, Ce) (**2**).[6e,f] Time-resolved absorption spectroscopic investigations revealed that the unprecedented $M_2@(I_h\text{-}C_{80})^{\bullet+}$–$(ZnP)^{\bullet-}$ radical ion pair was produced in polar solvents (benzonitrile and DMF), while the $(M_2)^{\bullet-}@I_h$-C_{80}–$(ZnP)^{\bullet+}$ radical ion pair was produced in less polar solvents (toluene and THF). More recently, it was demonstrated that $La_2@I_h$-C_80 acts as a pure electron donor both in nonpolar and polar media when combined with the electron accepting 11,11,12,12-tetracyano-9,10-anthra-*p*-quinodimethane (TCAQ) (**3**).[6i] Lately, a non-covalent coordinative D–A hybrid composed of zinc tetraphenylporphyrin (ZnP) and a pyridyl-appended $La_2@I_h$-C_{80} (**4**) has been reported.[6j]

To date, limited examples of EMF-based electron D–A conjugates put limitation on a comprehensive understanding of the photophysical properties of EMFs. In view of designing new electron D–A conjugates, chemical stability of the corresponding radical ion pair species is imperative. In this respect, heteroaromatics such as 10-methylphenothiazine and 10-methylphenoxazine are known as excellent electron donors due to their ability to form stable radical cations.[8] Such heteroaromatics exhibit low ionization potentials, which are additional criteria for efficient solar conversion schemes.

In this report, we describe the synthesis of a novel $La_2@I_h$-C_{80}-based electron D–A conjugate (**5**) by attaching an electron donating POZ and the photophysical

characteristics by means of time-resolved absorption spectroscopy. We also investigated the photophysics of **4** as a reference, because spectroscopic signatures of any states of the $La_2@I_h$-C_{80} moiety in **5** are more similar to $La_2@I_h$-C_{80} with the same exohedral functionalization, i.e. **4**, than pristine $La_2@I_h$-C_{80}.

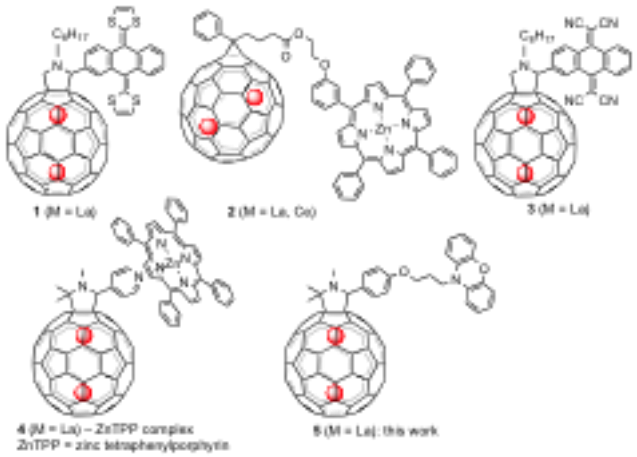

Figure 1. $M_2@I_h$-C_{80}-based electron D–A conjugates **1**–**5**.

Results and Discussion

Scheme 1 illustrates the synthetic route towards conjugate **5**. In particular, the so-called "Prato reaction",[9] namely the 1,3-dipolar cycloadditions of in-situ generated azomethine ylides to fullerenes, was employed. $La_2@I_h$-C_{80}, *N*-substituted POZ-containing aldehyde **6**, and 2-methyl-2-(methylamino)propanoic acid were heated under reflux in toluene for 3 h. Analytical high-performance liquid chromatography (HPLC) afforded a new peak for the reaction mixture. Product **5** was formed in a regioselective manner (see Figure S1 in the ESI) and isolated by preparative HPLC using a Buckyprep column. The yield was 75% based on consumed $La_2@I_h$-C_{80}. Evidence for formation of **5** came from a matrix-assisted laser desorption ionization–time-of-flight (MALDI–TOF) mass spectrum with a peak at *m*/*z* 1639.

From Figure S5 we note that two different types of carbon–carbon bonds are available in $La_2@I_h$-C_{80} for the reaction with azomethine ylides. On one hand, it is the bond that bisects two hexagons, that is, a [6,6]-junction, and, on the other hand, it is the bond that bisects a pentagon and a hexagon, that is, a [5,6]-junction. In addition, when considering the POZ moiety, four substitution patterns are possible for **5**. Although both ^{1}H and ^{13}C NMR spectra of **5** – Figures S6 and S7

– fail to provide structural insights as far as the C_1 symmetry is concerned, they turned out to be useful for verifying the purity of **5**. In both spectra only a single set of NMR signals are discernible. For example, 75 out of 78 signals in the ^{13}C NMR spectrum are assignable to the sp^2 cage carbons. In addition, the two signals appeared at 63.8 and 66.5 ppm are ascribable to the sp^3 cage carbons.

Evidence for the [5,6]-addition pattern comes from the absorption spectra of **5** and of other $La_2@I_h$-C_{80}-based pyrrolidinofullerenes. Firstly, a distinctive absorption maximum centered at around 687 nm was seen for [6,6]-$La_2@C_{80}(CH_2)_2NTrt$, which is characteristic of the [6,6]-pyrrolidino $M_2@I_h$-C_{80} isomer. Secondly, no characteristic features were noted in the absorption spectrum of the corresponding [5,6]-pyrrolidino $M_2@I_h$-C_{80} isomer [5,6]-$La_2@C_{80}(CH_2)_2NTrt$ (see Figure S9).[10]

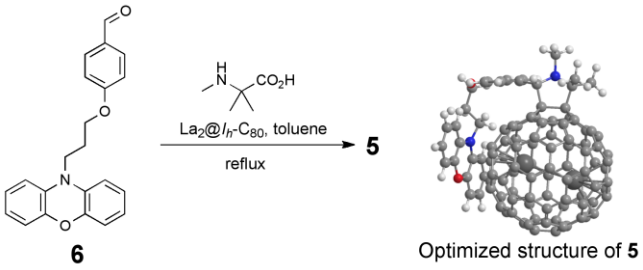

Scheme 1. Synthesis of conjugate **5** and its optimized structure.

The electrochemical features of **4**, **5**, and the corresponding references in the form of cyclic (CV) and differential pulse voltammetry (DPV) are illustrated in Figures S10 and S11, respectively, and are summarized in Table 1. Importantly, subtle differences characterize the redox potentials of the [6,6]- and [5,6]-$La_2@C_{80}(CH_2)_2NTrt$ isomers.[10b] In this context, the redox potentials of **5** more closely resemble those of [5,6]-$La_2@C_{80}(CH_2)_2NTrt$, which further supports our conclusion that a [5,6]-addition pattern is present in **5**. The first oxidation of **5** corresponds to the overlapping oxidations of POZ and the pyrrolidine.

Table 1. Redox Potentials[a] of **4–6** and Corresponding References

Compound	$^{ox}E_2$	$^{ox}E_1$	$^{red}E_1$
4	+0.56	+0.16[d]	–0.52
5	+0.53	+0.14[d,e]	–0.49
6	N/A	+0.22	N/A
[5,6]-$La_2@I_h$-$C_{80}(CH_2)_2NTrt$[b]	+0.63	+0.23	–0.45
[6,6]-$La_2@I_h$-$C_{80}(CH_2)_2NTrt$[b]	+0.95	+0.55	–0.51
$La_2@I_h$-C_{80}[c]	+0.95	+0.56	–0.31

[a] All of the potentials, in volts, were measured relative to the ferrocene/ferrocenium couple and were obtained by DPV. [b] Ref. 10b. [c] Ref. 7a. [d] Irreversible. [e] Two-electron oxidation process.

The results of theoretical calculations as depicted in Scheme 1 and Figure S19 suggest a folded conformation for **5**. As such, POZ and $La_2@I_h$-C_{80} must be assumed to be in close proximity to each other.[11] Decisive for the effective formation of the $(La_2@I_h\text{-}C_{80})^{\bullet-}$-$(POZ)^{\bullet+}$ radical ion pair state is the fact that the distributions of the POZ-centered HOMO and the endohedral M_2-centered LUMO are well separated – Figure S20.

The electrochemical oxidation of POZ and reduction of **4** to form the radical cation of POZ and the radical anion of **4**, respectively, was probed in spectroelectrochemical experiments. This was deemed important to assign the differential absorption changes. In terms of reduction of **4**, a broad maximum at around 1215 nm as well as weaker minima at 835 and 960 nm emerged as characteristics as shown in Figure 2a.[6j] In addition, the radical anion species of **4** has distinct maxima at 512, 572, 605, and 772 nm as well as a minimum at 674 nm. In terms of oxidation of POZ, the differential absorption spectra following the conclusion of the spectroelectrochemical oxidation in deaerated 1,2-dichlorobenzene (1,2-DCB) reveal maxima at 411 and 544 nm as shown in Figure 2b.

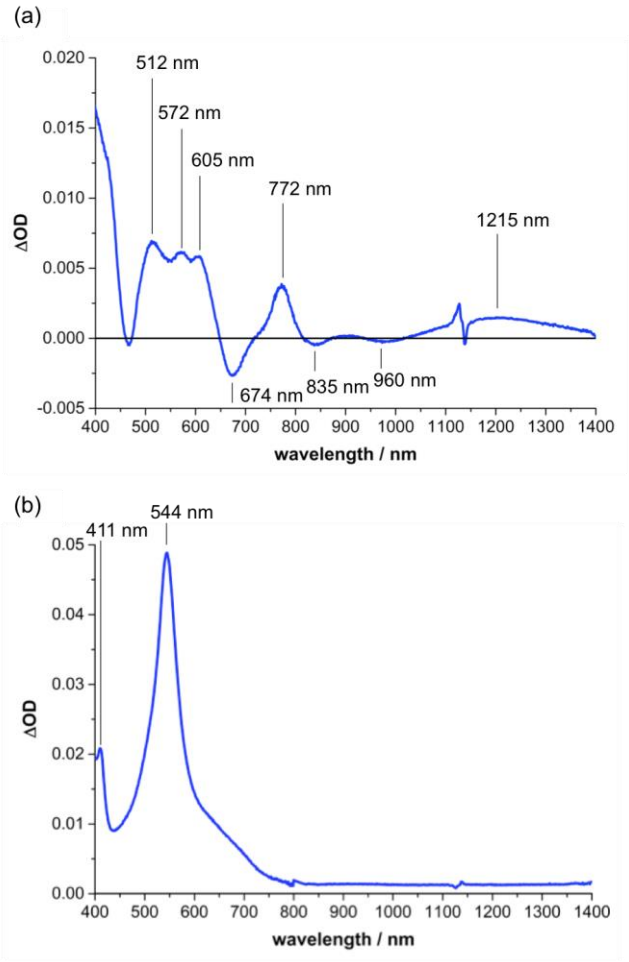

Figure 2. (a) Differential absorption spectra (visible and near-infrared) obtained upon electrochemical reduction of **4** at an applied bias of −0.5 V in argon-saturated 1,2-DCB at room temperature. (b) Differential absorption spectra (visible and near-infrared) obtained upon electrochemical oxidation of POZ at an applied bias of +0.5 V in argon-saturated 1,2-DCB at room temperature.

Excited state events of the $La_2@I_h$-C_{80} and POZ moieties in **5** following femtosecond and nanosecond excitation were investigated by means of transient absorption measurements. Figure 3 shows the differential absorption changes of POZ upon excitation at 387 nm. These include strong maxima at 500 and 685 nm, which relate to the singlet excited state of POZ. In POZ, the singlet excited state decays via intersystem crossing with a lifetime of 1.5 ± 0.1 ns to afford the corresponding triplet excited state. For the latter, transient maxima are registered at 465 and 535 nm.

In reference to Figure 4, we note that for **4**, photo-excitation at 387 nm leads to appreciable ground state bleaching at 465 nm. This bleaching is accompanied by a rather well-resolved fine structure with maxima at 515, 566, 614, 800, and 900 nm. Notably, $La_2@I_h$-C_{80} has a closed-shell character. Still, its singlet excited state is rather short-lived with a lifetime of 45 ± 5 ps. A heavy-atom effect seems a plausible rationale as it facilitates the spin-orbit coupling and, in turn, the intersystem crossing. Commencing with the singlet-excited-state decay, a weak and broad absorption in the 800–1200 nm range, along with broad features that taper at 550 nm, develops. The latter relates to the triplet excited state of $La_2@I_h$-C_{80}, which is formed from efficient intersystem crossing, in accordance with literature reports.[6i,12]

Either 387 or 420 nm laser pulses exclusively address the $La_2@I_h$-C_{80} singlet excited state due to the lack of any POZ absorption at these excitation wavelengths as shown in Figure S12. Conjugate **5** reveals, right after the conclusion of the 387 nm excitation – Figures 5 and S13–S15 – differential absorption changes in the form of transient maxima at 512, 565, 610, 800, and 900 nm as well as a transient minimum at 465 nm. We assign these changes to the $La_2@I_h$-C_{80} singlet excited state (1.4 ± 0.2 eV) in good agreement with the experiments with **4**.[6k]

It is not the slow intersystem crossing, which populates the corresponding triplet excited state in **5**. Instead, the $La_2@I_h$-C_{80} singlet excited state decays ultrafast with solvent dependent lifetimes of 6.4 ± 0.6 ps in toluene, 2.1 ± 0.5 ps in THF, and 0.7 ± 0.3 ps in benzonitrile, as shown in Figures S16, and S17.

Simultaneously with the singlet excited state decay, new transitions develop in the visible and near-infrared region of spectrum on a timescale of a few picoseconds. At first glance, maxima are seen at 512, 535, 565, 610, 700, 800 nm and a broad near-infrared tail. A closer look reveals that the maximum at 535 nm bears resemblance with the spectroelectrochemical findings regarding the POZ radical cation – $POZ^{\bullet+}$. The visible region, in contrast, as well as a broad near-infrared tail is attributable to the $La_2@I_h$-C_{80} radical anion – $(La_2@I_h\text{-}C_{80})^{\bullet-}$. Taking the aforementioned into concert, we conclude that an energetically $(La_2@I_h\text{-}C_{80})^{\bullet-}$-$(POZ)^{\bullet+}$ low-lying radical ion pair state (0.63 eV) is formed via ultrafast through-space electron transfer. Both fingerprints were

employed as reliable probes for the lifetime determination of the $(La_2@I_h\text{-}C_{80})^{\bullet-}$-$(POZ)^{\bullet+}$ radical ion pair state. From a global analysis, charge recombination lifetimes of 96 ± 7, 63 ± 8, and 101 ± 35 ps were determined in toluene, THF, and benzonitrile, respectively. Solvent dependency for the biphasic $La_2@I_h\text{-}C_{80}$ singlet excited state decay in **5** clearly underpins our assignments of charge separation and charge recombination.

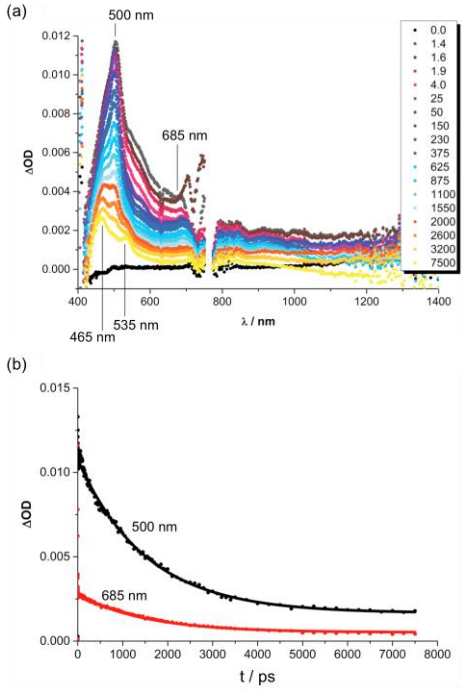

Figure 3. (a) Differential absorption spectra (visible and near-infrared) obtained upon femtosecond flash photolysis (387 nm) of POZ (10^{-5} M) in argon-saturated THF with several time delays between 0 and 7500 ps at room temperature. (b) Time-absorption profiles of the spectra shown above at 500 (black) and 685 nm (red) monitoring the intrinsic intersystem crossing.

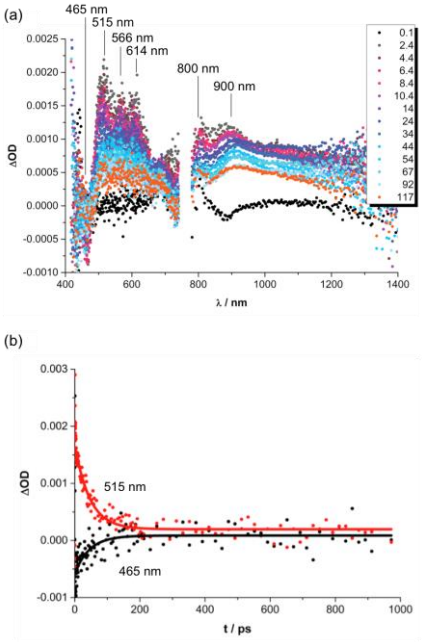

Figure 4. (a) Differential absorption spectra (visible and near-infrared) obtained upon femtosecond flash photolysis (387 nm) of **4** (10^{-5} M) in argon-saturated toluene with several time delays between 0 and 117 ps at room temperature. (b) Time-absorption profiles of the spectra shown above at 465 (black) and 515 nm (red) monitoring the intrinsic intersystem crossing.6k

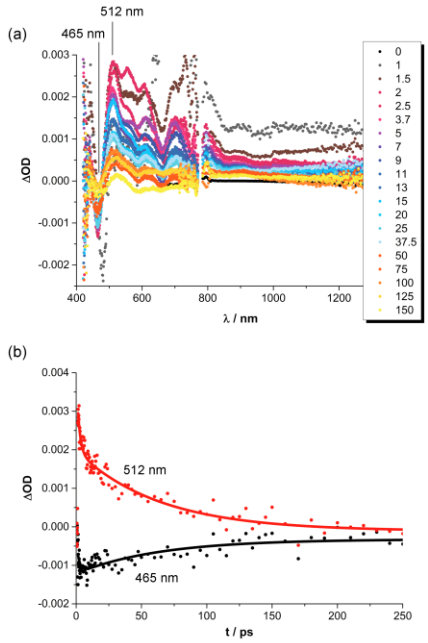

Figure 5. (a) Differential absorption spectra (visible and near-infrared) obtained upon femtosecond flash photolysis (387 nm) of **5** (10^{-5} M) in argon-saturated THF with several time delays between 0 and 150 ps at room temperature. (b) Time-absorption profiles of the spectra shown above at 465 (black) and 512 nm (red) monitoring the charge separation and charge recombination.

Table 2. Characteristic Absorption Spectral Change

POZ	Absorption maximum (nm)
Radical cation[a]	411, 544
Singlet excited state[b]	500, 685
Triplet excited state[b]	465, 535

Conjugate **4**	Absorption maximum (nm)	Absorption minimum (nm)
Radical anion[a]	512, 572, 605, 772, 1215 (broad)	674, 835, 960
Singlet excited state[b]	515, 566, 614, 800, 900	465
Triplet excited state[b]	550 (broad), NIR (broad)	

Conjugate **5**	Absorption maximum (nm)	Absorption minimum (nm)
Singlet excited state[b]	512, 565, 610, 800, 900	465
Radical anion ($(La_2@I_h\text{-}C_{80})^{\bullet-}$)[b]	512, 565, 610, 800, 900, NIR tail	
Radical cation ($(POZ)^{\bullet+}$)[b]	535	

[a] Electrochemically generated. [b] Excited at 387 nm.

Conclusions

In short, we have prepared a new electron donor-acceptor conjugate featuring $La_2@I_h\text{-}C_{80}$ as an electron acceptor and POZ as an electron donor, respectively, by exploiting Prato conditions. The reaction took place preferably at the [5,6]-junction to allow regioselective formation of conjugate **5**. Computational calculations suggest a folded conformation for **5**, in which the POZ moiety is in

close proximity to the fullerene cage. Corroboration for the formation of the $(La_2@I_h\text{-}C_{80})^{\bullet-}$-$(POZ)^{\bullet+}$ radical ion pair state came from time-resolved absorption spectroscopic studies. Throughout, we conclude that electron transfer upon photo-excitation is governed by a through-space mechanism. Though the presented charge separated state lifetime of the conjugate is short, this investigation provides a new insight for the excited state characteristics of EMF-based electron donor-acceptor conjugates.

Experimental Section

N-substituted POZ-containing aldehyde **6**[13] and $La_2@I_h\text{-}C_{80}$[14] were synthesized according to literature procedures.

Synthesis of **5**. A mixture of $La_2@I_h\text{-}C_{80}$ (1.0 mg, $8.1 \cdot 10^{-4}$ mmol), **6** (14 mg, $4.1 \cdot 10^{-2}$ mmol, 50 eq.) and 2-methyl-2-(methylamino)propanoic acid (10 mg, $8.5 \cdot 10^{-2}$ mmol, 10^5 eq.) in toluene (20 mL) was placed in a pyrex tube. After degassing by three freeze–pump–thaw cycles under reduced pressures, the mixture was heated to reflux under Ar for 3 h. The mixture was filtered through a membrane filter (pore size, 0.45 mm) and the solvent was removed using a rotary evaporator. The residue was dissolved in toluene and injected into a preparative HPLC to allow isolation of **5**. Pure **5** was obtained as a brown solid (Yield, 75% based on consumed $La_2@I_h\text{-}C_{80}$, determined using HPLC).

Data for **5**. ^{1}H NMR (500 MHz, in CS_2 ([D6]acetone capillary as lock solvent; 293 K) δ 6.95–7.00 (m, 1H; Ar-$H^{E'}$), 6.65–6.68 (m, 1H; Ar-H^{E}), 6.32–6.35 (m, 1H; Ar-$H^{F'}$), 6.15 (dd, J = 2.0, 8.3 Hz, 1H; Ar-H^{F}), 5.95 (dt, J = 1.2, 7.6 Hz, 2H; Ar-H^{K}), 5.75–5.85 (m, 6H; Ar-$H^{J, L, M}$), 3.60 (s, 1H; CH^{D}), 3.44 (t, J = 5.5 Hz, 2H; OCH^{I}_2), 3.06 (t, J = 7.5 Hz, 2H; NCH^{G}_2), 1.72 (s, 3H; NCH^{C}_3), 1.45–1.50 (m, 2H; CH^{H}_2), 1.32 (s, 3H; CH^{B}_3), 0.84 (s, 3H; CH^{A}_3) ppm; ^{13}C NMR (125 MHz in CS2 ([D6]acetone capillary as lock solvent); 293 K) δ 159.01 (C_e), 154.74, 152.94, 150.76, 149.30, 148.76, 148.23, 147.43, 146.70, 146.56, 146.19, 145.89, 145.31, 144.89 (C^g), 144.78, 144.70, 144.65, 144.60, 144.55, 144.03, 143.96, 143.42, 143.26, 143.21, 142.91, 142.86, 142.81, 142.10, 142.01, 141.89, 141.48, 141.26, 141.14, 141.04, 140.93, 140.54, 140.45, 140.40, 140.32, 140.15, 140.08, 140.00, 139.88, 139.81, 139.69, 139.65, 139.02, 138.96, 138.92, 138.89, 138.74, 138.37, 138.30, 138.10, 137.90, 137.69, 137.63, 137.28, 137.20, 136.79, 136.64, 136.50,

136.46, 136.39, 136.23, 136.12, 135.94, 135.67, 135.24, 135.18, 134.35, 133.01 (C^{d}), 132.90, 131.91 ($C^{E'}H$), 130.58 ($C^{E}H$), 129.80, 129.30, 129.25 (C^{f}), 128.99, 128.60, 124.06 ($C^{K}H$), 122.86, 121.55 ($C^{L}H$), 115.89 ($C^{J}H$), 115.10 ($C^{F'}H$), 113.70 ($C^{F}H$), 111.44 ($C^{M}H$), 81.97 ($C^{D}H$), 72.43 (C^{a}), 66.32 (C^{b}), 65.33 ($OC^{G}H_2$), 63.93 (C^{c}), 41.08 ($NC^{I}H_2$), 32.17 ($NC^{C}H_3$), 26.28 ($C^{B}H_3$), 26.18 ($C^{H}H_3$), 16.43 ($C^{A}H_3$) ppm, 97 resonances out of 100 ones due to peak overlap; MALDI-TOF MS (TPB): *m*/*z*: 1639 ([*M*]$^-$), 1238 ([*M* – $C_{26}H_{28}N_2O_2$]$^-$).

Stability of **5**. When pure **5** was heated at 120°C for 2h, retrocycloaddition took place and the gradual formation of pristine $La_2@I_h$-C_{80} was observed. When the retrocycloaddition was conducted in the presence of *N*-phenylmaleimide, formation of the corresponding 1,3-dipolar cycloadduct (**7**, see Figure S4) of the 1,3-azomethine ylide intermediate and *N*-phenylmaleimide was observed in the MALDI-TOF mass spectrum (see Figures S3, S4). As such, Martín et al. have reported similar retrocycloadditions of fulleropyrrolidines and endohedral fulleropyrrolidines.15

Acknowledgements

This work was supported by a Grant-in-Aid for Scientific Research on Innovative Areas (Grant 20108001, “pi-Space”), a Grant-in-Aid for Scientific Research (A) (Grant 202455006) and (B) (No. 24350019), Specially Promoted Research (Grant 22000009) from the Ministry of Education, Culture, Sports, Science, and Technology of Japan.

Keywords: fullerenes • electrochemistry • photo-induced electron transfer • transient absorption spectroscopy

[1] H. Imahori, Y. Sakata, *Adv. Mater.* **1997**, *9*, 537–546; (b) D. Gust, T. A. Moore, *Acc. Chem. Res.* **2001**, *34*, 40–48; (c) N. S. Lewis, D. G. Nocera, *Proc. Natl. Acad. Sci. U. S. A.* **2006**, *103*, 15729–15735. (d) G. Bottari, G. de la Torre, D. M. Guldi, T. Torres, *Chem. Rev.* **2010**, *110*, 6768–6816; (e) M. Frank, J. Ahrens, I. Bejenke, M. Krick, D. Schwarzer, G. H. Clever, *J. Am. Chem. Soc.* **2016**, *138*, 8279–8287.

[2] (a) L. Echegoyen, L. E. Echegoyen, *Acc. Chem. Res.* **1998**, *31*, 593–601; (b) F. Arias, L. Echegoyen, S. R. Wilson, Q. Lu, Q. Lu, *J. Am. Chem. Soc.* **1995**, *117*, 1422–1427; (c) L. Echegoyen, F. Diederich, L. E. Echegoyen in *Fullerenes: Chemistry, Physics, and Technology* (Eds.: K. M. Kadish, R. S. Ruoff),

John Wiley & Sons, New York, **2000**, pp 1–53.

[3] (a) T. D. Anthopoulos, B. Singh, N. Marjanovic, N. S. Sariciftci, A. M. Ramil, H. Sitter, M. Cölle, D. M. de Leeuw, *Appl. Phys. Lett.* **2006**, *89*, 213504; (b) P. Moreno-García, A. La Rosa, V. Kolivoska, D. Bermejo, W. Hong, K. Yoshida, M. Baghernejad, S. Filippone, P. Broekmann, T. Wandlowski, N. Martín, *J. Am. Chem. Soc.* **2015**, *137*, 2318–2327.

[4] (a) H. Imahori, D. M. Guldi, K. Tamaki, Y. Yoshida, C. Luo, Y. Sakata, S. Fukuzumi, *J. Am. Chem. Soc.* **2001**, *123*, 6617–6628; (b) K. Ohkubo, H. Kotani, J. Shao, Z. Ou, K. M. Kadish, G. Li, R. K. Pandey, M. Fujitsuka, O. Ito, H. Imahori, S. Fukuzumi, *Angew. Chem. Int. Ed.* **2004**, *43*, 853–856; (c) D. M. Guldi, H. Imahori, K. Tamaki, Y. Kashiwagi, H. Yamada, Y. Sakata, S. Fukuzumi, *J. Phys. Chem. A* **2004**, *108*, 541–548; (d) H. Imahori, Y. Sekiguchi, Y. Kashiwagi, T. Sato, Y. Araki, O. Ito, H. Yamada, S. Fukuzumi, *Chem. –Eur. J.* **2004**, *10*, 3184–3196; (e) (f) T. Hasobe, *J. Phys. Chem. Lett.* **2013**, *4*, 1771–1780.

[5] (a) *Endofullerenes: A New Family of Carbon Clusters* (Eds.: T. Akasaka, S. Nagase), Kluwer Academic Publishers, Dordrecht, **2002**; (b) M. N. Chaur, F. Melin, A. L. Ortiz, L. Echegoyen, *Angew. Chem. Int. Ed.* **2009**, *48*, 7514–7538; (c) X. Lu, L. Feng, T. Akasaka, S. Nagase, *Chem. Soc. Rev*. **2012**, *41*, 7723–7760.

[6] (a) J. R. Pinzón, M. E. Plonska-Brzezinska, C. M. Cardona, A. J. Anthans, S. S. Gayathri, D. M. Guldi, M. Á. Herranz, N. Martín, T. Torres, L. Echegoyen, *Angew. Chem. Int. Ed.* **2008**, *47*, 4173–4176; (b) R. B. Ross, C. M. Cardona, D. M. Guldi, S. G. Sankaranarayanan, M. O. Reese, N. Kopidakis, J. Peet, B. Walker, G. C. Bazan, E. Van Keuren, B. C. Holloway, M. Drees, *Nat. Mater.* **2009**, *8*, 208–212; (c) J. R. Pinzón, D. C. Gasca, S. G. Sankaranarayanan, G. Bottari, T. Torres, D. M. Guldi, L. Echegoyen, *J. Am. Chem. Soc*. **2009**, *131*, 7727–7734; (d) Y. Takano, M. Á. Herranz, N. Martín, S. G. Radhakrishnan, D. M. Guldi, T. Tsuchiya, S. Nagase, T. Akasaka, *J. Am. Chem. Soc.* **2010,** *132*, 8048–8055; (e) D. M. Guldi, L. Feng, S. G. Radhakrishnan, H. Nikawa, M. Yamada, N. Mizorogi, T. Tsuchiya, T. Akasaka, S. Nagase, M. Á. Herranz, N. Martín, *J. Am. Chem. Soc.* **2010**, *132*, 9078–9086; (f) L. Feng, S. G. Radhakrishnan, N. Mizorogi, Z. Slanina, H. Nikawa, T. Tsuchiya, T. Akasaka, S. Nagase, N. Martín, D. M. Guldi, *J. Am. Chem. Soc.* **2011**, *133*, 7608–7618; (g) B. Grimm, J. Schornbaum, C. M.

Cardona, J. D. van Paauwe, P. D. W. Boyd, D. M. Guldi, *Chem. Sci.* **2011**, *2*, 1530–1537; (h) S. Wolfrum, J. R. Pinzón, A. Molina-Ontoria, A. Gouloumis, N. Martín, L. Echegoyen, D. M. Guldi, *Chem. Commun.* **2011**, *47*, 2270–2272; (i) Y. Takano, S. Obuchi, N. Mizorogi, R. García, R.; M. Á. Herranz, M. Rudolf, S. Wolfrum, D. M. Guldi, N. Martín, S. Nagase, T. Akasaka, *J. Am. Chem. Soc.* **2012**, *134*, 19401–19408; (j) M. Rudolf, S. Wolfrum, D. M. Guldi, L. Feng, T. Tsuchiya, T. Akasaka, L. Echegoyen, *Chem. –Eur. J.* **2012**, *18*, 5136–5148; (k) T. Tsuchiya, M. Rudolf, S. Wolfrum, S. G. Radhakrishnan, R. Aoyama, Y. Yokosawa, A. Oshima, T. Akasaka, S. Nagase, D. M. Guldi, *Chem. –Eur. J*. **2013**, *19***,** 558–565; (l) M. Rudolf, S. V. Kirner, D. M. Guldi, Chem. Soc. Rev. 2016, 45, 612–630.

[7] (a) T. Suzuki, Y. Maruyama, T. Kato, K. Kikuchi, Y. Nakao, Y. Achiba, K. Kobayashi, S. Nagase, *Angew. Chem., Int. Ed. Engl.* **1995**, *34*, 1094–1096; (b) M. Yamada, T. Nakahodo, T. Wakahara, T. Tsuchiya, Y. Maeda, T. Akasaka, M. Kako, K. Yoza, E. Horn, N. Mizorogi, K. Kobayashi, S. Nagase, *J. Am. Chem. Soc.* **2005**, *127*, 14570–14571.

[8] (a) V. Biju, S. Barazzouk, K. G. Thomas, M. V. George, P. V. Kamat, *Langmuir* **2001**, *17*, 2930–2936; (b) D. G. Nocera, H. B. Gray, *J. Am. Chem. Soc.* **1981**, *103*, 7349–7350; (c) P. P. Infelta, M. Graetzel, J. H. Fendler, *J. Am. Chem. Soc.* **1980**, *102*, 1479–1483; (d) L. N. Domelsmith, L. L. Munchausen, K. N. Houk, *J. Am. Chem. Soc.* **1977**, *99*, 6506–6514; (e) Y. Moroi, A. M. Braun, M. Graetzel, *J. Am. Chem. Soc.* **1979**, *101*, 567–572; (f) M. Sakaguchi, M. Hu, L. Kevan, *J. Phys. Chem.* **1990**, *94*, 870–874; (g) J. N. Younathan, W. E. Jones Jr., T. J. Meyer, *J. Phys. Chem.* **1991**, *95*, 488–492; (h) Q.-X. Guo, Z.-X. Liang, B. Liu, S.-D. Yao, Y.-C. Liu, *J. Photochem. Photobiol. A* **1996**, *93*, 27–31.

[9] M. Maggini, G. Scorrano, M. Prato, *J. Am. Chem. Soc.* **1993**, *115*, 9798–9799.

[10] (a) M. Yamada, T. Wakahara, T. Nakahodo, T. Tsuchiya, Y. Maeda, T. Akasaka, K. Yoza, E. Horn, N. Mizorogi, S. Nagase, *J. Am. Chem. Soc.* **2006**, *128*, 1402–1403; (b) M. Yamada, M. Okamura, S. Sato, C. I. Someya, N. Mizorogi, T. Tsuchiya, T. Akasaka, T. Kato, S. Nagase, *Chem. –Eur. J.* **2009**, *15*, 10533–10542.

[11] We recently calculated the relative energies for four possible isomers of conjugate **4**, where the POZ-linked phenyl was replaced by a pyridyl, and found

that the [5,6]-adduct with the pyridyl group on the pentagon side was the thermodynamically most favored isomer (ref. 6k). Accordingly, it is reasonable to assume that **5** is thermodynamically most favored among the four possible isomers. Therefore, we identify that **5** is the [5,6]-adduct with the POZ-linked phenyl substituent on the pentagon side.

[12] S. Nagase, K. Yamamoto, T. Kato, T. Wakahara, T. Akasaka, *Chem. Lett.* **2000**, *29*, 902–903.

[13] K. G. Thomas, V. Biju, P. V. Kamat, M. V. George, D. M. Guldi, *ChemPhysChem* **2003**, *4*, 1299–1307.

[14] K. Yamamoto, H. Funasaka, T. Takahashi, T. Akasaka, T. Suzuki, Y. Maruyama, *J. Phys. Chem.* **1994**, *98*, 12831–12833.

[15] (a) N. Martín, M. Altable, S. Filippone, Á. Martín-Domenech, L. Echegoyen, C. M. Cardona, *Angew. Chem. Int. Ed*. **2006**, *45*, 110–114; (b) S. Filippone, M. I. Barroso, Á. Martín-Domenech, S. Osuna, M. Solà, N. Martín, *Chem. –Eur. J.* **2008**, *14*, 5198–5206.

Entry for the Table of Contents

FULL PAPER

A newly designed electron donor–acceptor conjugate consisting of an endohedral dimetallofullerene (La2@*Ih*-C80) and phenoxazine (POZ) was successfully synthesized by exploiting Prato conditions. Time-resolved absorption spectroscopic investigations corroborate the formation of the energetically low-lying radical ion pair state via ultrafast through-space electron transfer.

T. Akasaka, A. Nakata, M. Rudolf, W.-W. Wang, M. Yamada, M. Suzuki, Y. Maeda, R. Aoyama, T. Tsuchiya, S. Nagase, D. M. Guldi**

Page No. – Page No.

Synthesis and Photo-Induced Electron Transfer Reactions in a $La_2@I_h$-C_{80}–Phenoxazine Conjugate